

**Breakdown of the Migdal-Eliashberg theory: A determinant quantum Monte Carlo study**I. Esterlis,<sup>1</sup> B. Nosarzewski,<sup>1,2</sup> E. W. Huang,<sup>1,2</sup> B. Moritz,<sup>2</sup> T. P. Devereaux,<sup>2,3</sup> D. J. Scalapino,<sup>4</sup> and S. A. Kivelson<sup>1,3</sup><sup>1</sup>*Department of Physics, Stanford University, Stanford, California 94305, USA*<sup>2</sup>*Stanford Institute for Materials and Energy Sciences, SLAC National Accelerator Laboratory and Stanford University, Menlo Park, California 94025, USA*<sup>3</sup>*Geballe Laboratory for Advanced Materials, Stanford University, Stanford, California 94305, USA*<sup>4</sup>*Department of Physics, University of California, Santa Barbara, California 93106-9530, USA*

(Received 7 November 2017; revised manuscript received 19 February 2018; published 2 April 2018)

The superconducting (SC) and charge-density-wave (CDW) susceptibilities of the two-dimensional Holstein model are computed using determinant quantum Monte Carlo, and compared with results computed using the Migdal-Eliashberg (ME) approach. We access temperatures as low as 25 times less than the Fermi energy,  $E_F$ , which are still above the SC transition. We find that the SC susceptibility at low  $T$  agrees quantitatively with the ME theory up to a dimensionless electron-phonon coupling  $\lambda_0 \approx 0.4$  but deviates dramatically for larger  $\lambda_0$ . We find that for large  $\lambda_0$  and small phonon frequency  $\omega_0 \ll E_F$  CDW ordering is favored and the preferred CDW ordering vector is uncorrelated with any obvious feature of the Fermi surface.

DOI: [10.1103/PhysRevB.97.140501](https://doi.org/10.1103/PhysRevB.97.140501)

**Introduction.** The electron-phonon (e-p) problem is of broad importance in solid-state physics, and especially so in the theory of superconductivity (SC). In this context, a key question is what are the conditions that lead to the highest possible SC transition temperature,  $T_c$ . Given that this occurs when the dimensionless e-p coupling  $\lambda_0$  is not small, one would *a priori* expect this question might be analytically unanswerable. However, Migdal-Eliashberg (ME) theory purports to be valid even if  $\lambda_0$  is not small, provided  $\lambda_0\omega_0/E_F$  is small, where  $\omega_0$  is an average phonon frequency and  $E_F$  is the Fermi energy [1,2]. On the other hand, from a strong-coupling (large  $\lambda_0$ ) perspective, it is clear ME theory breaks down for large  $\lambda_0$  no matter how small  $\omega_0/E_F$ , due to the formation of bipolarons [3–5]. Thus, one faces the practical question: at what value of the e-p coupling does ME theory break down, and how?

**Model.** To be explicit, we consider the two-dimensional Holstein Hamiltonian [6]

$$H = H_e + H_p + H_{ep}, \quad (1)$$

where

$$H_e = - \sum_{ij,\sigma} t_{ij} (c_{i\sigma}^\dagger c_{j\sigma} + \text{H.c.}) - \mu \sum_{i,\sigma} n_{i\sigma},$$

$$H_p = \sum_i \left( \frac{P_i^2}{2M} + \frac{1}{2} K X_i^2 \right),$$

$$H_{ep} = \alpha \sum_{i,\sigma} n_{i,\sigma} X_i, \quad (2)$$

$c_{i\sigma}^\dagger$  creates an electron on site  $i$  with spin polarization  $\sigma = \uparrow, \downarrow$ ,  $n_{i\sigma} = c_{i\sigma}^\dagger c_{i\sigma}$  is the local electronic density,  $P_i$  and  $X_i$  are the position and momentum operators of Einstein phonons with mass  $M$ , and  $\mu$  is the chemical potential. The bare phonon frequency is thus  $\omega_0 = \sqrt{K/M}$ , and  $\alpha$  is the e-p coupling constant. (We take units in which  $M = \hbar = k_B = 1$ .)

There are two important dimensionless parameters in the model: the adiabatic parameter  $\omega_0/E_F$  and the dimensionless e-p coupling

$$\lambda_0 = \alpha^2 \rho(E_F)/K, \quad (3)$$

where  $\rho(E_F)$  is the density of states at the Fermi energy. To make contact with other approaches we also present data as a function of a “renormalized” coupling, denoted by  $\lambda$ , which we define in analogy with the phenomenological coupling extracted from tunneling spectra and often used in studies of “strongly coupled” superconductors [7]. In the limit of weak coupling,  $\lambda = \lambda_0 + O(\lambda_0^2)$ , but for  $\lambda_0 \sim 1$ , we will see that phonon softening leads to  $\lambda > \lambda_0$ . The prescription for computing  $\lambda$  will be explained below in Eq. (9).

We investigate this model numerically via determinant quantum Monte Carlo (DQMC) simulations and analytically via ME theory. Details of the DQMC algorithm, including explanation of both the local and global phonon field updates used, can be found in [8]. Unless stated otherwise, we work with a square lattice with both nearest-neighbor and next-nearest-neighbor hopping  $t'/t = -0.3$  and a fixed density  $n = 0.8$ . We keep a nonzero  $t'$  to avoid nesting near half-filling and also because previous studies have found that nonzero  $t'$  leads to an enhanced pairing response [9]. We have studied systems of linear size  $L = 8-12$  with periodic boundary conditions and temperatures  $T = \beta^{-1} = t/4$  to  $t/16$ . All data in the main text is shown for our largest system size  $L = 12$ , which is large enough that most observables are essentially  $L$  independent, i.e., are characteristic of the thermodynamic limit. The DQMC results are shown as solid symbols in the various figures and where error bars are not visible, the statistical error is less than the symbol size. The figures also show comparisons of the DQMC results with ME theory, which is shown as either continuous curves or open symbols. ME calculations have also been carried out on system size  $L = 12$ . All data in the main text has the adiabatic ratio  $\omega_0/E_F = 0.1$ , which puts

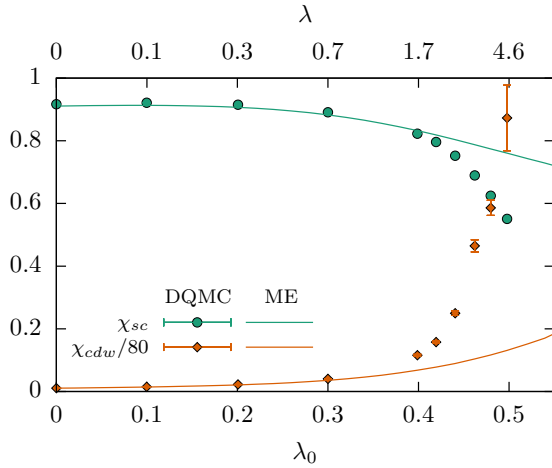


FIG. 1.  $\chi_{sc}$  and  $\chi_{cdw}$  as a function of  $\lambda_0$  (lower scale) and  $\lambda$  (upper scale) for  $\omega_0/E_F = 0.1$  at base temperature,  $\beta t = 16$ , density  $n = 0.8$ , and  $L = 12$ . Data points are DQMC values; solid lines are computed in ME approximation. We see a breakdown in the ME theory for  $\lambda_0 \gtrsim 0.4$  ( $\lambda \gtrsim 1.7$ ).

us comfortably within the putative regime of validity of ME theory. In the Supplemental Material [10] we present data for other values of  $\omega_0/E_F$ . We note that this model is free of the notorious minus-sign problem and hence we are able to access relatively large system sizes and low temperatures. However, for the parameters used here, we are still unable to access temperatures  $T \lesssim t/16$  due to prohibitively long phonon autocorrelation times [11].

**Results.** While we typically cannot access sufficiently low temperatures to observe transitions to either a SC or a charge-density wave (CDW) phase, we do access low enough  $T$  that a significant growth of the corresponding susceptibilities can be measured, showing the ordering tendencies of the system. The  $s$ -wave pair susceptibility is defined as

$$\chi_{sc} = \int_0^\beta d\tau \langle \Delta(\tau) \Delta^\dagger(0) \rangle, \quad (4)$$

where

$$\Delta^\dagger = \frac{1}{L} \sum_i c_{i\uparrow}^\dagger c_{i\downarrow}^\dagger \quad (5)$$

and the CDW susceptibility is

$$\chi_{cdw}(\mathbf{q}) = \int_0^\beta d\tau \langle \rho_{\mathbf{q}}(\tau) \rho_{\mathbf{q}}^\dagger(0) \rangle, \quad (6)$$

where

$$\rho_{\mathbf{q}}^\dagger = \frac{1}{L} \sum_{i,\sigma} e^{i\mathbf{q}\cdot\mathbf{R}_i} c_{i\sigma}^\dagger c_{i\sigma}. \quad (7)$$

We will use the symbol  $\chi_{cdw}$  to represent the value of  $\chi_{cdw}(\mathbf{q})$  evaluated at  $\mathbf{q} \equiv \mathbf{Q}_{\max}$  at which it is maximal.

In Fig. 1 we plot  $\chi_{sc}$  and  $\chi_{cdw}$  as a function of  $\lambda_0$  (lower axis) and  $\lambda$  (upper axis) at the lowest studied temperature  $\beta t = 16$ . The results from the ME theory, discussed in more detail in the next section, agree quantitatively with the data for  $\lambda_0 \leq 0.4$  ( $\lambda \lesssim 1.7$ ), after which the SC susceptibility takes a sharp downturn while the ME theory shows no similar

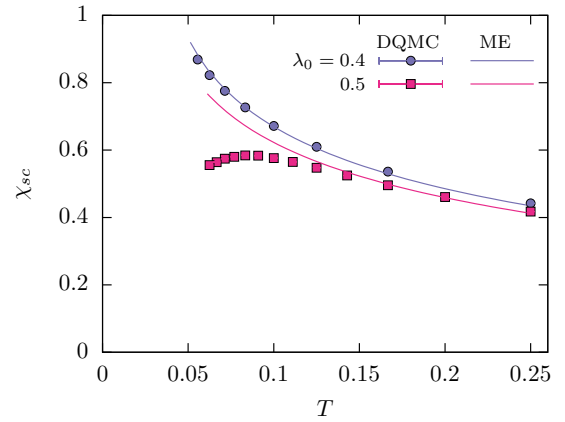


FIG. 2.  $\chi_{sc}$  as a function of  $T$  for fixed values of  $\lambda_0 = 0.4$  and  $0.5$  ( $\lambda \approx 1.7$  and  $4.6$ ),  $\omega_0/E_F = 0.1$ ,  $n = 0.8$ , and  $L = 12$ . For  $\lambda_0 = 0.4$ , the ME theory accurately captures the behavior of  $\chi_{sc}$  over the entire temperature range while for  $\lambda_0 = 0.5$  the theory is qualitatively incorrect.

features. We thus conclude that, for the parameters considered, ME theory breaks down dramatically for  $\lambda_0 \gtrsim 0.4$ . This is consistent with dynamical mean-field theory (DMFT) results reported by Bauer *et al.* [4], where it was found that the ME predictions differ from those of DMFT for  $\lambda_0 \gtrsim 0.3$ – $0.4$ . Also evident from Fig. 1 is that the downturn in  $\chi_{sc}$  is accompanied by a rapid rise of CDW correlations, which in turn leads to phonon softening and a corresponding increase in  $\lambda/\lambda_0$ . We find that  $\chi_{cdw}$  is peaked at wave vector  $\mathbf{Q}_{\max} = (\pi, \pi)$  which, we emphasize, is a wave vector not associated with any obvious features of the Fermi surface (see inset of Fig. 3 for the Fermi surface and Fig. S1 of the Supplemental Material for details about  $\chi_{cdw}$ ). The abrupt nature of the breakdown of ME theory can also be seen in Fig. 2, where we plot  $\chi_{sc}$  as a function of  $T$  for  $\lambda_0 = 0.4, 0.5$  ( $\lambda \approx 1.7, 4.6$ ). For  $\lambda_0 = 0.4$ , ME theory shows good agreement with the data over the entire temperature range  $\beta t = 4$ – $16$ . However, for  $\lambda_0 = 0.5$ , while the ME theory does predict a decrease in the pairing response relative to  $\lambda_0 = 0.4$ , it clearly misses even the qualitative behavior of  $\chi_{sc}$ .

We have also computed the electron and phonon imaginary time ordered Green's functions. In Fig. 3 we plot the imaginary part of the electronic self-energy  $\text{Im}\Sigma$  for  $\lambda_0 = 0.2, 0.4$ , and  $0.5$  ( $\lambda \approx 0.3, 1.7, 4.6$ ), as a function of Matsubara frequency  $\omega_n = (2n + 1)\pi T$  and for two momenta near the Fermi surface. For  $\lambda_0 = 0.2$  the self-energy is nearly momentum independent and the Matsubara frequency dependence of  $\text{Im}\Sigma$  is captured accurately by ME theory. For  $\lambda_0 = 0.4$  the self-energy develops weak momentum dependence and the dependence on both  $\mathbf{k}$  and  $\omega_n$  is again captured well by ME theory. For  $\lambda_0 = 0.5$  the self-energy remains weakly momentum dependent in both the ME and DQMC results but ME theory drastically underestimates the magnitude of the self-energy.

In Fig. 4 we plot the renormalized phonon frequency  $\Omega(\mathbf{q}, 0) = [\omega_0^2 + \Pi(\mathbf{q}, 0)]^{1/2}$ , where  $\Pi(\mathbf{q}, \nu_n)$  is defined implicitly in terms of the phonon Green's function according to

$$D(\mathbf{q}, \nu_n) \equiv \frac{2\omega_0}{(i\nu_n)^2 - \omega_0^2 - \Pi(\mathbf{q}, \nu_n)} \quad (8)$$

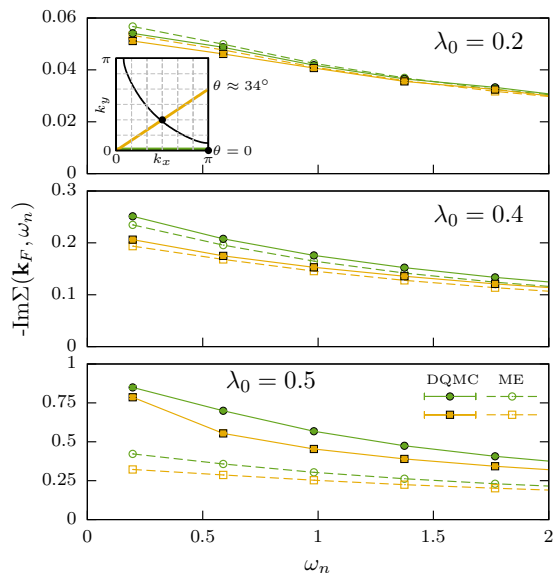


FIG. 3. Imaginary part of the electronic self-energy,  $\text{Im}\Sigma(\mathbf{k} \approx \mathbf{k}_F, \omega_n)$ , where  $\omega_n = (2n + 1)\pi T$  and  $\mathbf{k} \approx \mathbf{k}_F$  is a momentum near the Fermi surface, evaluated at  $\theta = 0$  and  $\theta \approx 34^\circ$ . The inset shows the  $\mathbf{k}$ -space mesh for an  $L = 12$  grid and the two points at which  $\text{Im}\Sigma$  is evaluated. These points correspond to the points closest to the zone diagonal and zone boundary, respectively, of the Fermi surface. The ME theory captures both the Matsubara frequency and momentum dependence of  $\text{Im}\Sigma$  for  $\lambda_0 \leq 0.4$  but again shows a breakdown for  $\lambda_0 = 0.5$ . Other parameters are  $\omega_0/E_F = 0.1$ ,  $\beta t = 16$ ,  $n = 0.8$ , and  $L = 12$ .

and  $\nu_n = 2\pi nT$ . For  $\lambda_0 = 0.2$  and  $0.4$  we see that the ME theory captures the renormalization of the phonon propagator with remarkable accuracy. (For  $\lambda_0 = 0.4$ , there is a noticeable error in the ME result in a narrow range of  $\mathbf{q}$  around  $(\pi, \pi)$ ; this reflects an emerging problem in treating the CDW tendencies, as is discussed further in the Supplemental Material.) However, for  $\lambda_0 = 0.5$ , ME theory drastically underestimates (by a factor

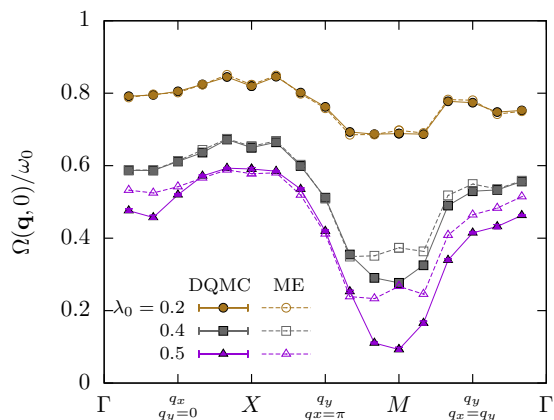


FIG. 4. Ratio of renormalized to bare phonon frequency. The renormalized phonon frequency is defined in Eq. (8). For  $\lambda_0 \leq 0.4$  we see ME theory accurately predicts the momentum dependence of  $\Omega(\mathbf{q}, 0)$ . However, for  $\lambda_0 = 0.5$ , ME theory dramatically underestimates the softening of the phonon propagator at  $\mathbf{q} = (\pi, \pi)$ . Other parameters are  $\omega_0/E_F = 0.1$ ,  $n = 0.8$ ,  $\beta t = 16$ , and  $L = 12$ .

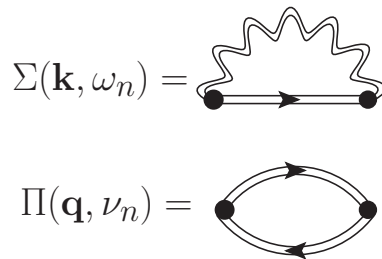


FIG. 5. Migdal equations for electronic and phonon self-energies in the normal state. Double lines indicate fully renormalized Green's functions and the solid dot is the bare vertex  $\alpha$ .

of  $\sim 3$ ) the phonon softening at  $\mathbf{q} = (\pi, \pi)$  and also gives a weaker softening near  $\mathbf{q} = 0$ .

*Migdal-Eliashberg theory.* The ME theory for the normal state of an interacting e-p system can be summarized by the diagrams in Fig. 5, which constitute a set of closed self-consistent equations for the electron and phonon self-energies. The approach is justified by the observation that the leading correction to the e-p vertex is proportional to  $\omega_0/E_F$ , and hence can be ignored for  $\omega_0/E_F \ll 1$  [1,2]. As pointed out in [12], it is important to include self-consistently the equation for the phonon self-energy (rather than just using the bare phonon propagator in the electron self-energy equation) to account for effects due to phonon softening near a CDW transition. Details of the numerical procedure used to solve these equations and how the self-energies are used to compute various observables can be found in, e.g., [12,13].

An important quantity entering the ME theory is the coupling constant  $\lambda$  [7], defined as

$$\lambda = 2 \int_0^\infty d\omega \frac{\alpha^2 F(\omega)}{\omega}, \quad (9)$$

where  $\alpha^2 F(\omega) = \rho(E_F) \alpha^2 \langle B(\mathbf{k} - \mathbf{k}', \omega) \rangle_{\text{FS}}$ . Here  $B(\mathbf{q}, \omega)$  is the phonon spectral function and the brackets denote the Fermi surface (FS) average

$$\begin{aligned} \langle B(\mathbf{k} - \mathbf{k}', \omega) \rangle_{\text{FS}} &= \frac{1}{\rho(E_F)^2} \int \frac{d^2\mathbf{k}}{(2\pi)^2} \frac{d^2\mathbf{k}'}{(2\pi)^2} \\ &\times B(\mathbf{k} - \mathbf{k}', \omega) \delta(\epsilon_{\mathbf{k}} - E_F) \delta(\epsilon_{\mathbf{k}'} - E_F). \end{aligned} \quad (10)$$

To extract this quantity from DQMC data we use the relationship between the imaginary time ordered phonon Green's function and the spectral function,

$$D(\mathbf{q}, \nu_n) = \int_0^\infty d\omega B(\mathbf{q}, \omega) \frac{2\omega}{(i\nu_n)^2 - \omega^2}, \quad (11)$$

from which it follows that

$$\lambda = -\frac{\lambda_0 \omega_0}{2} \langle D(\mathbf{k} - \mathbf{k}', 0) \rangle_{\text{FS}}. \quad (12)$$

*Conclusions.* Comparing the DQMC results on the Holstein model with ME theory, we find remarkably good quantitative agreement for e-p coupling less than a crossover value,  $\lambda_0 \lesssim \lambda^* = 0.4$ . However, as  $\lambda_0$  exceeds  $\lambda^*$ , increasingly dramatic quantitative and qualitative differences develop. This is despite the fact that  $\lambda(\bar{\Omega}/E_F)$  (the nominal control parameter for ME

theory) is still small, and that the ME theory shows no sign that a crossover has occurred. (Note that while  $\lambda$  increases over  $\lambda_0$ , the average phonon frequency  $\bar{\Omega}$  decreases so that at  $\lambda_0 = 0.5$ ,  $\lambda\bar{\Omega}/E_F \approx 0.3$ .) This crossover appears in some ways analogous to a first-order transition; it involves a change in the character of the low-energy theory to one which will eventually (at larger  $\lambda_0$ ) be governed by the strong-coupling physics of bipolarons, commensurate CDWs, and phase separation [3–5].

Our results are also interesting in the context of the quest for higher  $T_c$  superconductors. For  $\lambda_0 \lesssim \lambda^*$ , the measured  $\chi_{sc}$  agrees well with ME theory in the accessible range of temperatures, and hence it is reasonable to use the ME expression as a way to extrapolate the DQMC results to lower  $T$ . By this line of reasoning, we can use the value of  $T_c$  computed within ME as a reliable estimate of the true  $T_c$  for  $\lambda_0$  in this range. Since the ME  $T_c$  is an increasing function of  $\lambda_0$  we conclude the same is true of the actual  $T_c$ , so long as  $\lambda_0 \lesssim \lambda^*$ . On the other hand, for  $\lambda_0 = 0.5$  (where ME theory no longer agrees with the DQMC results),  $\chi_{sc}$  from DQMC is a decreasing function of decreasing temperature (see Fig. 2), from which we conclude  $T_c$  has been substantially suppressed and likely vanishes. This implies  $T_c$  is optimized around  $\lambda_0 \approx \lambda^*$ , where from ME theory we estimate that the maximal  $T_c$  is  $T_c^{(max)} \approx 8 \times 10^{-2} \omega_0$ .

The property of an optimal  $T_c$  should be contrasted with conventional ME theory, which predicts a monotonically increasing  $T_c$  as a function of  $\lambda_0$  [14,15]. Of course, it is likely that the precise value of  $\lambda^*$  is nonuniversal, and there may be ways to engineer the model to increase it further; say, by suppressing the CDW and/or polaronic tendencies. For instance, Pickett [16] has discussed the possibility of using multiple quasi-2D Fermi surfaces to enhance  $T_c$  and Werman and Berg [17] have recently shown that in a particular large  $N$  limit, in which the number of phonon modes is large compared to the number of fermionic modes, one can access the large  $\lambda$  limit without polaronic effects. However, as seen in  $H_3S$  [18,19], it is probably a more promising route to increase  $T_c$  by increasing  $\omega_0$  (the prefactor in  $T_c$ ) keeping  $\lambda_0 \approx \lambda^*$ , rather than increasing  $\lambda$  [20–22]. (On the other hand, increasing  $\omega_0$  makes the effects of bare Coulomb repulsion—which are completely absent in our treatment—more important.)

Finally, our results should be put in the context of previous studies of the Holstein model. The competition between SC and CDW has been studied via DQMC, albeit with a different focus and in a different parameter regime (see [9,12,13,23], and references therein). The Holstein model has also been studied extensively via DMFT (see [4,24–29] for discussions of the crossover between weak and strong coupling as well as assessments of the validity of ME theory for the Holstein model). The conclusions of these studies are broadly similar to those reached here, in that discrepancies between ME theory and DMFT appear for relatively small values of  $\lambda_0$ , where there is an onset of phonon softening and a significant increase in the renormalized coupling  $\lambda$ . However, because the DMFT is done in infinite dimensions, we are unable to make quantitative comparisons with these studies. Using the dynamical cluster approximation, the inclusion of lowest-order vertex corrections has been studied [30]. In that study it was found that inclusion of vertex corrections tends to return the system to the ME regime by averting phonon softening. As we have seen, however, the ME theory already underestimates the phonon softening, suggesting that the inclusion of vertex corrections will not save the theory.

*Acknowledgments.* We would like to thank Akash Maharaj, Raghu Mahajan, and Abolhassan Vaezi for collaboration during early stages of this work. We acknowledge insightful discussions with Sri Raghu, Samuel Lederer, and Yoni Schattner. I.E., B.N., E.W.H. B.M., and T.P.D. were supported by the US Department of Energy, Office of Basic Energy Sciences, Division of Materials Sciences and Engineering, under Contract No. DE-AC02-76SF00515. S.A.K. was supported by NSF DMR-1608055. D.J.S. was supported by the Scientific Discovery through Advanced Computing (SciDAC) program funded by US Department of Energy, Office of Science, Advanced Scientific Computing Research and Basic Energy Sciences, Division of Materials Sciences and Engineering. This research was supported in part by the National Science Foundation under Grant No. NSF PHY11-25915. Computational work was performed on the SIMES and Sherlock clusters at Stanford University.

- 
- [1] A. Migdal, *Sov. Phys. JETP* **7**, 996 (1958).
  - [2] G. Eliashberg, *Sov. Phys. JETP* **11**, 696 (1960).
  - [3] A. S. Alexandrov, *Europhys. Lett.* **56**, 92 (2001).
  - [4] J. Bauer, J. E. Han, and O. Gunnarsson, *Phys. Rev. B* **84**, 184531 (2011).
  - [5] E. W. Carlson, V. J. Emery, S. A. Kivelson, and D. Orgad, *Concepts in High Temperature Superconductivity*, in *Superconductivity: Conventional and Unconventional Superconductors*, edited by K. H. Bennemann and J. B. Ketterson (Springer, Berlin, Heidelberg, 2008), pp. 1225–1348.
  - [6] T. Holstein, *Ann. Phys. (NY)* **8**, 325 (1959).
  - [7] P. B. Allen and B. Mitrović, in *Solid State Physics*, edited by H. Ehrenreich, F. Seitz, and D. Turnbull (Academic, New York, 1983), Vol. 37, pp. 1–92.
  - [8] S. Johnston, E. A. Nowadnick, Y. F. Kung, B. Moritz, R. T. Scalettar, and T. P. Devereaux, *Phys. Rev. B* **87**, 235133 (2013).
  - [9] M. Vekić, R. M. Noack, and S. R. White, *Phys. Rev. B* **46**, 271 (1992).
  - [10] See Supplemental Material at <http://link.aps.org/supplemental/10.1103/PhysRevB.97.140501> for details of the CDW and other values of the adiabatic ratio.
  - [11] M. Hohenadler and T. C. Lang, *Computational Many-Particle Physics* (Springer, New York, 2008), pp. 357–366.
  - [12] F. Marsiglio, *Phys. Rev. B* **42**, 2416 (1990).
  - [13] R. T. Scalettar, N. E. Bickers, and D. J. Scalapino, *Phys. Rev. B* **40**, 197 (1989).
  - [14] P. B. Allen and R. C. Dynes, *Phys. Rev. B* **12**, 905 (1975).
  - [15] V. Z. Kresin, *Phys. Lett. A* **122**, 434 (1987).
  - [16] W. E. Pickett, *J. Supercond. Novel Magn.* **19**, 291 (2006).

- [17] Y. Werman and E. Berg, *Phys. Rev. B* **93**, 075109 (2016).
- [18] N. W. Ashcroft, *Phys. Rev. Lett.* **21**, 1748 (1968).
- [19] A. P. Drozdov, M. I. Erements, I. A. Troyan, V. Ksenofontov, and S. I. Shylin, *Nature (London)* **525**, 73 (2015).
- [20] C. Lin, B. Wang, and K. H. Teo, *Phys. Rev. B* **93**, 224501 (2016).
- [21] C. Grimaldi, L. Pietronero, and S. Strässler, *Phys. Rev. Lett.* **75**, 1158 (1995).
- [22] J. E. Han, O. Gunnarsson, and V. H. Crespi, *Phys. Rev. Lett.* **90**, 167006 (2003).
- [23] R. M. Noack, D. J. Scalapino, and R. T. Scalettar, *Phys. Rev. Lett.* **66**, 778 (1991).
- [24] J. K. Freericks, M. Jarrell, and D. J. Scalapino, *Phys. Rev. B* **48**, 6302 (1993).
- [25] J. K. Freericks, *Phys. Rev. B* **48**, 3881 (1993).
- [26] D. Meyer, A. C. Hewson, and R. Bulla, *Phys. Rev. Lett.* **89**, 196401 (2002).
- [27] J. P. Hauge and N. d'Ambrumenil, *J. Low Temp. Phys.* **151**, 1149 (2008).
- [28] P. Benedetti and R. Zeyher, *Phys. Rev. B* **58**, 14320 (1998).
- [29] M. Capone and S. Ciuchi, *Phys. Rev. Lett.* **91**, 186405 (2003).
- [30] J. P. Hauge, *J. Phys.: Condens. Matter* **15**, 2535 (2003).